

**Microsolvation**

# Adaptive Response to Solvation in Flexible Molecules: Oligo Hydrates of 4-Hydroxy-2-butanone

 Meng Li<sup>†</sup>, Wenqin Li<sup>†</sup>, Cristóbal Pérez, Alberto Lesarri,\* and Jens-Uwe Grabow\*

**Abstract:** Structural changes induced by water play a pivotal role in chemistry and biology but remain challenging to predict, measure, and control at molecular level. Here we explore size-governed gas-phase water aggregation in the flexible molecule 4-hydroxy-2-butanone, modeling the conformational adaptability of flexible substrates to host water scaffolds and the preference for sequential droplet growth. The experiment was conducted using broadband rotational spectroscopy, rationalized with quantum chemical calculations. Two different isomers were observed experimentally from the di- to the pentahydrates (4-hydroxy-2-butanone-(H<sub>2</sub>O)<sub>n=2-5</sub>), including the <sup>18</sup>O isotopologues for the di- and trihydrates. Interestingly, to accommodate water molecules effectively, the heavy atom skeleton of 4-hydroxy-2-butanone reshapes in every observed isomer and does not correspond to the stable conformer of the free monomer. All solvates initiate from the alcohol group (proton donor) but retain the carbonyl group as secondary binding point. The water scaffolds closely resemble those found in the pure water clusters, balancing between the capability of 4-hydroxy-2-butanone for steering the orientation and position of the water molecules and the ability of water to modulate the monomer's conformation. The present work thus provides an accurate molecular description on how torsionally flexible molecules dynamically adapt to water along progressing solvation.

Water is ubiquitous on Earth and indispensable for sustaining life. Accordingly, a plethora of water-related studies are found across the realms of chemistry, biology and atmospheric sciences.<sup>[1-3]</sup> Among them, gas-phase studies of water aggregation play a unique role describing the structure and energetics of size-governed clusters and the chemical evolution from the monohydrates to the formation of nanodroplets.<sup>[4-11]</sup> This molecular research is experimentally challenging, but contributes to the models bridging the gap between the interactions in small-clusters and the description of solvated biomolecules and liquids.<sup>[12]</sup> Water clusters reveal the balance between the monomers' internal bonding forces determining the shape of the unsolvated molecule and the much weaker non-covalent interactions (NCIs) competing in molecular complexation vs. water self-aggregation. While NCIs associated with water have long been a focal point of research,<sup>[13]</sup> the subsequent water-induced alterations in molecular structure are both intriguing and neither totally explored nor understood. Known examples include the water influence on protein folding<sup>[14,15]</sup> and protein-ligand binding.<sup>[16,17]</sup> However, assessing the role of water in the conformational behavior of large biomolecules is still difficult to control, observe, and predict. The solvation of small molecules in size-specific aqueous environments can provide fundamental insight on the water's ability to induce structural alterations, providing experimentally conclusive evidence to validate, complement and benchmark the computational predictions.

The structure and NCIs of molecules and clusters can be determined through microwave spectroscopy, at a precision offered by no other spectroscopic method.<sup>[18-21]</sup> However, despite the wealth of rotational studies, most of them are limited to only one or two water molecules,<sup>[21]</sup> hiding the view of the accumulative structural changes along the successive addition of water molecules. Moreover, previous studies are mostly limited to substrates with low conformational variability. Nevertheless, the development of broadband microwave techniques<sup>[19,20]</sup> made the observation of a few larger hydrates in the range of  $n = 3-6$  water molecules, severely obstructed by weak and congested spectra, feasible. For most of these larger clusters, water molecules create self-association networks resembling the corresponding pure water clusters, then named *droplet* aggregation.<sup>[22-24]</sup> Evidence for this aggregation pattern has also been obtained through IR studies, as in benzene-(H<sub>2</sub>O)<sub>n=6-8</sub>.<sup>[25-27]</sup> In a few cases, e.g., the di- to pentahydrate water clusters of 3-methylcatechol (MC-(H<sub>2</sub>O)<sub>n=2-5</sub>),<sup>[28]</sup> the aggregate structure is visibly different from the pure water clusters, thus termed

[\*] M. Li,<sup>†</sup> Prof. Dr. J.-U. Grabow  
 Institut für Physikalische Chemie & Elektrochemie, Gottfried-  
 Wilhelm-Leibniz-Universität  
 Callinstr. 3 A, 30167 Hannover (Germany)  
 E-mail: jens-uwe.grabow@pci.uni-hannover.de

W. Li,<sup>†</sup> Dr. C. Pérez, Prof. Dr. A. Lesarri  
 Departamento de Química Física y Química Inorgánica, Facultad  
 de Ciencias—IU CINQUIMA, Universidad de Valladolid  
 Paseo de Belén, 7, 47011 Valladolid (Spain)  
 E-mail: alberto.lesarri@uva.es

[†] These authors contributed equally to this work.

© 2024 The Authors. Angewandte Chemie International Edition published by Wiley-VCH GmbH. This is an open access article under the terms of the Creative Commons Attribution Non-Commercial NoDerivs License, which permits use and distribution in any medium, provided the original work is properly cited, the use is non-commercial and no modifications or adaptations are made.

wetting pathway. These two pathways show how different solute species may govern solvent aggregation. Indeed, the aggregation pattern is quite dependent on the solute monomer structure. With the conformational space being low-dimensional, structural changes are deemed to be rather small or just subtle for rigid solutes. For the benzaldehyde-water clusters  $\text{BA}-(\text{H}_2\text{O})_{n=1-6}$ , the dihedral angle between the phenyl ring and the  $-\text{CHO}$  group of BA changed less than 10 degrees compared with the free monomer.<sup>[23]</sup> For the 3-methyl-3-oxetanemethanol-water clusters  $\text{MOM}-(\text{H}_2\text{O})_{n=1-6}$ , in which the monomer bears a flexible alicyclic rather than a rigid aromatic ring, the angle of the oxetane ring puckers within 25 degrees.<sup>[22]</sup> Hydration governed puckering also stabilizes the high energy conformers of the 12-crown-4 ether.<sup>[29]</sup> In the  $n=1-6$  water clusters of the two-carbon molecule of glycoaldehyde (GLY), the heavy atom backbone of the monomer rotates out of plane between 53 and 90 degrees.<sup>[24]</sup> Interestingly, the elongation of larger molecular backbones or lateral chains, as reported on the small clusters of methyl lactate-water ( $\text{ML}-(\text{H}_2\text{O})_{n=1,2}$ ),<sup>[30]</sup> 2-aminoethanol-water ( $\text{AE}-(\text{H}_2\text{O})$ ),<sup>[31]</sup> serotonin- $(\text{H}_2\text{O})_{n=1,2}$ ,<sup>[32]</sup> or tetrahydro-2-turoic acid-water,<sup>[33]</sup> show the strong potential of flexible molecules to undergo significant structural changes. However, with the size of the water clusters increasing, the spectroscopic identification of isomeric structures becomes progressively challenging. Growing complexity arises from multiple structures which may only differ in the orientations of the endocyclic hydrogen bonds (HBs) of the water cluster, as observed in the  $\text{BA}-(\text{H}_2\text{O})_{n=4-6}$  aggregates.<sup>[23]</sup> Consequently, acquiring the structure of a water cluster, them concertively governing an  $n$ -dimensional conformational behavior of a flexible molecule with complicated potential energy surfaces (PES), represents a rather intricate experimental endeavor.

4-Hydroxy-2-butanone (4H2B) features both hydrophilic alcohol and carbonyl groups separated by two methylene units, so it is expected to display a rich conformational behavior. A preceding rotational study on the monomer and its monohydrate showed water disrupting the intramolecular HB within 4H2B, but led to small changes in the monomer, characterized by a *gauche* alcohol group ( $\tau(\text{C9C10-C11O12})$  ca.  $65-70^\circ$ , for the atom numbering see Figure 2).<sup>[34]</sup> Here, we will prove that, unlike in rigid molecules, the introduction of 2 to 5 water molecules in a flexible open-chain carbon skeleton will engage water scaffolds with the internal torsional motions of 4H2B, leading to monomer adaptation as the hydrate grows. This work will thus offer an unique high-resolution and size-dependent view of the competing intra- and intermolecular solvation interactions, mimicking water interactions on large biologically functional molecules. At the same time, the interplay between monomer and solvated structures of 4H2B will reveal aggregation patterns fundamentally different to those of rigid substrates, illustrating how the monomer or water may dominate solvation on increasingly larger complexes. The balance between energy costs and structural deformation on water aggregation makes also 4H2B a model for theoretical computations on solvation of flexible organic molecules.

The rotational spectra of the 4H2B monomer and its monohydrate were reported in our preceding study up to 20 GHz.<sup>[34]</sup> From this work, it was known that only a limited number of transitions are present below 8 GHz due to their relatively large values of the rotational constants. For this reason, the heavier di- to pentahydrates were recorded in the 2–8 GHz region using a broadband chirp-excitation Fourier transform microwave spectrometer<sup>[35,36]</sup> in Valladolid. The initial conformational search of  $4\text{H2B}-(\text{H}_2\text{O})_{n=2-5}$  used the semiempirical conformer-rotamer ensemble sampling tool CREST.<sup>[37]</sup> Further geometry optimizations were performed at the B3LYP-D3(BJ)/6-311++G(d,p)<sup>[38-41]</sup> level of theory. Afterwards, some of geometries were re-examined with the B2PLYP-D3(BJ)/def2TZVP<sup>[42-44]</sup> and RI-MP2/ aug-cc-pVTZ<sup>[45-47]</sup> methods. The calculations used Gaussian 16<sup>[48]</sup> and ORCA 5.0.<sup>[49]</sup> The theoretical results for all clusters are reported in Tables S1–S12. Furthermore, a relaxed PES scan was carried out at the B3LYP-D3(BJ)/6-311++G(d,p) level of theory. To provide more accurate deformation energies between the observed conformer of the free monomer and the 4H2B moiety in the hydrated structures, the respective single point energy calculations were also conducted at the same level. Full experimental and computational details are reported in the Supporting Information.

The spectral analysis was guided by the predicted geometries of the  $4\text{H2B}-(\text{H}_2\text{O})_{n=2-5}$  clusters, given in Tables S13–S23. Following a long iterative procedure which compared the spectrum to multiple molecular simulations for each cluster, the rotational transitions of the di- to pentahydrates were progressively identified. Illustrative sections of the spectrum are shown in Figure 1. Noticeably, two isomers were observed for each of the 4H2B aggregates comprising two to five water molecules.

The experimental spectroscopic parameters for all observed isomers of the  $4\text{H2B}-(\text{H}_2\text{O})_{n=2-5}$  clusters are reported in Table 1. The internal rotation barrier of the methyl group was not determined for all isomers, as only a small number of torsionally split transitions (*A* and *E* symmetry states) could be identified. Hence, the spectral observations were reproduced with a Watson's *S*-reduced semi-rigid rotational Hamiltonian,<sup>[50]</sup> including only *A* state transitions (Tables S24–S31). The lines of the resolved *E* state are summarized in Tables S32–S38, documenting the large fraction of overlaps with the *A* state. No *E* state and blended (overlapped by *A* and *E* state) lines were observed for  $4\text{H2B}-(\text{H}_2\text{O})_4\text{-II}$ , thus resulting in a smaller rms global deviation than for other isomers. The centrifugal distortion constants were partially determined for the present experimental data set. The unfitted centrifugal distortion constants were fixed at zero. The spectral assignments were also confirmed by observation of the  $\text{H}_2^{18}\text{O}$  isotopic species for the dihydrates  $4\text{H2B}-(\text{H}_2\text{O})_2\text{-II}$  and  $4\text{H2B}-(\text{H}_2\text{O})_2\text{-III}$  and the trihydrate  $4\text{H2B}-(\text{H}_2\text{O})_3\text{-I}$ , reported in Tables S39–S47. Based on the rotational constants of these isotopologues (Tables S48–S50), the coordinates of the water oxygen in  $4\text{H2B}-(\text{H}_2\text{O})_2\text{-II}$ ,  $4\text{H2B}-(\text{H}_2\text{O})_2\text{-III}$  and  $4\text{H2B}-(\text{H}_2\text{O})_3\text{-I}$  were derived with the Kraitchman's equations<sup>[51]</sup> (Tables S51–S53), allowing for a partial substitution ( $r_s$ ) structure

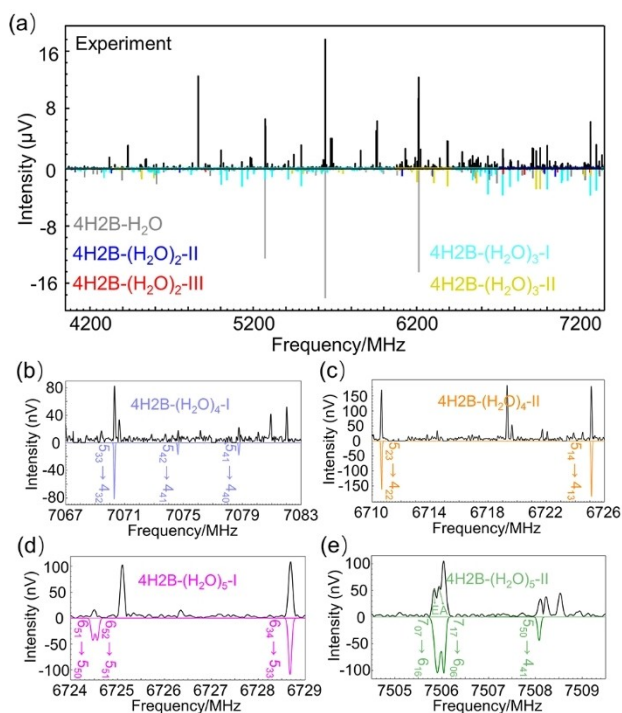


**Figure 1.** Sections of the broadband rotational spectra of 4H2B-(H<sub>2</sub>O)<sub>n=1-3</sub> (a), 4H2B-(H<sub>2</sub>O)<sub>4-I</sub> (b), 4H2B-(H<sub>2</sub>O)<sub>4-II</sub> (c), 4H2B-(H<sub>2</sub>O)<sub>5-I</sub> (d), and 4H2B-(H<sub>2</sub>O)<sub>5-II</sub> (e). The upper positive trace shows the experimental spectrum (after removal of the monomer transitions). The negative traces, in different colors, are the simulated spectra based on the fitted rotational parameters. The A and E torsional symmetry splittings due to the methyl internal rotation are illustrated for the transition 7<sub>0,7</sub>←6<sub>1,6</sub> of 4H2B-(H<sub>2</sub>O)<sub>5-II</sub> (e).

(Tables S54–S56). Effective structures<sup>[52]</sup> ( $r_0$ ) were also determined by a least-squares fit adjusting the vibrational ground rotational constants (Tables S54–S56). Finally, semi-experimental structures<sup>[53]</sup> ( $r_e^{SE}$ ) were determined from the corrected rotational constants (Table S60) in Tables S54–S56.

The structures of the di- and trihydrates of 4H2B are depicted in Figure 2 (a). Four plausible isomers were found on the PES of the dihydrate 4H2B-(H<sub>2</sub>O)<sub>2</sub> within 5 kJ mol<sup>-1</sup>, and two of them (II and III) were positively identified in the spectrum. The global minimum (isomer I) could not be assigned because of the small dipole moments and the reduced number of observable transitions. The isomers I (SI) and II of the dihydrate form characteristic water chains, inserting the two water molecules between the carbonyl and the alcohol sites of the monomer, with water acting as proton donor to the carbonyl group (acceptor to the alcohol), as in the monohydrate. Water insertion into isomers I and II requires a significant increase of the alcohol-to-carbonyl distance (monomer: 2.2 Å), leading to large torsional changes (ca. 80–130°) in the carbonyl dihedral  $\tau(O8C9-C10C11)$ . The theoretical dihedrals for the carbon skeleton and alcohol torsion of the 4H2B structure in the observed isomers are shown in Figure S1. The departure from the near-antiperiplanar carbon skeleton of the monomer and the monohydrate and a reorientation of the alcohol enlarges the alcohol-carbonyl distance in the dihydrate to 3.5–3.6 Å. The water chain is the preferred binding motif in other dihydrates like MOM-(H<sub>2</sub>O)<sub>2</sub>,<sup>[22]</sup> BA-(H<sub>2</sub>O)<sub>2</sub>,<sup>[23]</sup> GLY-(H<sub>2</sub>O)<sub>2</sub><sup>[24]</sup> and MC-(H<sub>2</sub>O)<sub>2</sub>.<sup>[28]</sup> Conversely, isomer III mostly retains the structure of the monohydrate, but uncommonly adding a second proton donor water molecule to the alcohol, which now behaves as bridge between the two water molecules. A comparison of the O...O water distances in the two isomers with the theoretical values in Tables S54 and S55 shows a ca. 8% decrease, suggesting cooperative effects.<sup>[4-9]</sup>

In the case of the trihydrate 4H2B-(H<sub>2</sub>O)<sub>3</sub>, the most stable isomers I and II in Figure 2(a) were detected in the experiment and the most intense one was unequivocally confirmed by isotopic substitution. In both isomers, the alcohol group serves as molecular anchor to build a closed ring of four consecutive hydroxyl groups, reminiscent of the pure water tetramer in Figure 2(b).<sup>[4]</sup> In addition, one of the water molecules (O3 in isomer I, O1 in isomer II) exerts a

**Table 1:** Experimental spectroscopic parameters of the 4H2B-(H<sub>2</sub>O)<sub>n=2-5</sub> clusters.

Parameters	4H2B-(H <sub>2</sub> O) <sub>2-II</sub>	4H2B-(H <sub>2</sub> O) <sub>2-III</sub>	4H2B-(H <sub>2</sub> O) <sub>3-I</sub>	4H2B-(H <sub>2</sub> O) <sub>3-II</sub>	4H2B-(H <sub>2</sub> O) <sub>4-I</sub>	4H2B-(H <sub>2</sub> O) <sub>4-II</sub>	4H2B-(H <sub>2</sub> O) <sub>5-I</sub>	4H2B-(H <sub>2</sub> O) <sub>5-II</sub>
A/MHz <sup>[a]</sup>	1869.1533(38) <sup>[b]</sup>	1696.009(79)	1401.2895(17)	1200.96036(88)	904.0922(19)	1101.643(69)	804.878(42)	766.5032(12)
B/MHz	1267.2790(15)	1276.8702(57)	961.6085(21)	988.6439(11)	740.4262(46)	693.6488(23)	587.9747(14)	658.8228(13)
C/MHz	947.5525(13)	1077.2089(49)	796.2891(21)	883.01517(70)	665.5203(39)	625.3962(25)	528.2762(17)	523.1678(12)
D <sub>J</sub> /kHz			0.478(62)		0.361(52)	0.166(28)	0.139(16)	0.127(16)
D <sub>JK</sub> /kHz	0.234(64)		-1.244(41)					0.0181(86)
D <sub>K</sub> /kHz	2.44(30)		2.040(54)				-0.0113(38)	
d <sub>1</sub> /kHz					-0.108(49)			
d <sub>2</sub> /Hz			-34.8(72)					
P <sub>aa</sub> /uÅ <sup>2</sup>	331	283	400	331	441	539	594	527
P <sub>bb</sub> /uÅ <sup>2</sup>	202	186	235	241	318	269	363	429
P <sub>cc</sub> /uÅ <sup>2</sup>	68	112	126	180	241	190	265	230
$ \mu /D$	$\mu_b > \mu_a$ , no $\mu_c$	$\mu_a$ , no $\mu_b$ and $\mu_c$	$\mu_a \approx \mu_c > \mu_b$	$\mu_c > \mu_a$ , no $\mu_b$	$\mu_a > \mu_c$ , no $\mu_b$	$\mu_a$ , no $\mu_b$ and $\mu_c$	$\mu_a > \mu_b$ , no $\mu_c$	$\mu_b > \mu_a$ , no $\mu_c$
N <sup>[c]</sup>	20	8	46	26	22	19	31	44
$\sigma$ /kHz <sup>[d]</sup>	15.1	13.2	13.1	15.6	18.9	5.2	11.9	14.7

[a] Rotational constants (A, B, C), centrifugal distortion constants (D, D<sub>JK</sub>, D<sub>K</sub>, d<sub>1</sub>, d<sub>2</sub>), planar moments (P<sub>aa</sub>, P<sub>bb</sub>, P<sub>cc</sub>) and electric dipole moment components ( $\mu_a$ ,  $\mu_b$ , and  $\mu_c$ ). [b] Standard errors in parentheses in units of the last digit. [c] Number of transitions in the fit. [d] RMS deviation of the fit.

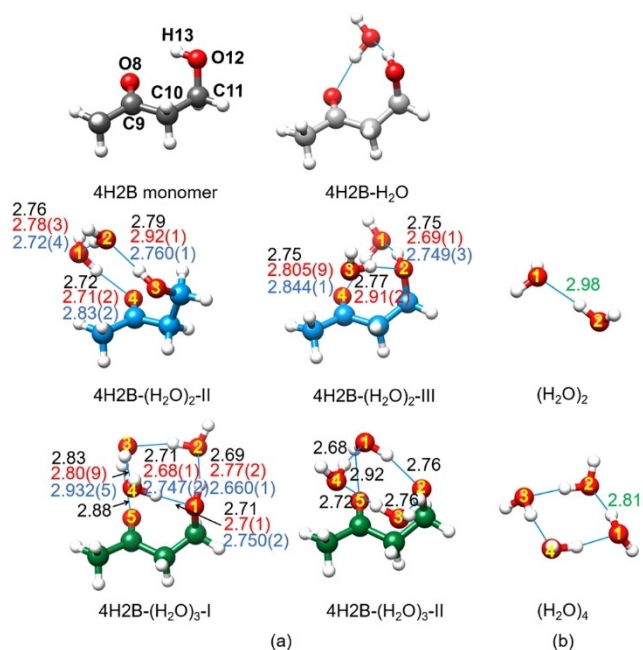


**Figure 2.** (a) The observed structures of 4H2B, 4H2B-H<sub>2</sub>O, 4H2B-(H<sub>2</sub>O)<sub>2</sub> and 4H2B-(H<sub>2</sub>O)<sub>3</sub>. The experimental  $r_s$  (blue) and  $r_0$  (red) O...O distances are compared with the theoretical values (B3LYP-D3(BJ))/6-311++G(d,p), (black). (b) The O...O distances (green) of the water dimer<sup>[6]</sup> and tetramer<sup>[4]</sup> are given for comparison.

role of double proton-donor, linking the water-alcohol network to a second binding site at the carbonyl group. The formation of a lateral OH-based square does not require large changes in the monomer, which is very similar in the two isomers and exhibits a near antiperiplanar carbon skeleton ( $\tau(\text{O8C9-C10C11})$  ca.  $\sim 24^\circ$ , for the atom numbering

see Figure 2). However, it is noticeably that a  $180^\circ$  rotation of the alcohol group permits the creation of both clockwise and anticlockwise orientations of the water units in the two isomers. In the pure water tetramer, the four free H atoms extend out of the water ring plane, adopting a symmetric up-down-up-down (u-d-u-d) orientation. This situation is replicated in both isomers with some distortions due to the interaction with the carbonyl group and some steric hindrance with 4H2B. The structural data for the O...O distances shown in Figure 2 and Table S56 reveal a slight ( $< \text{ca. } 5\%$ ) decrease relative to the average distance in the pure water tetramer (except O3...O4 in isomer I). In consequence, solvation of 4H2B up to the trihydrate confirms the decisive role of the functionalized polar groups as nucleation sites and how solvation proceeds by water self-aggregation to the molecular linking site, creating an initial nucleation droplet on top of the flexibly adapting monomer.

The PES of the tetrahydrate 4H2B-(H<sub>2</sub>O)<sub>4</sub> is much more complex, with 18 plausible isomers below  $5 \text{ kJ mol}^{-1}$ . Despite similarities in the rotational constants, the electric dipole moment components and the planar moments of inertia ( $P_{aa}$ ,  $P_{bb}$ , and  $P_{cc}$ ) permitted the assignment of isomers I and II (Figure 3 (a)) in the experiment. As the cluster size increases, some structural patterns recurrently emerge. First, for isomer I, we can clearly identify that water aggregation builds up from the alcohol group in 4H2B, which takes the structural role of a water molecule and forms a closed ring resembling the pure water pentamer of Figure 3 (b), characterized by a chiral asymmetric pentagon with coplanar oxygen atoms.<sup>[5]</sup> The H atoms in isomer I also adopt similar alternating orientations as those in the pure water pentamer (u-u-d-u-d), except for the water molecules establishing the second link to the carbonyl group. All differences in the O...O distances relative to the pure water pentamer are generally small (within  $\sim 0.2 \text{ \AA}$ ). However, the oxygen atoms

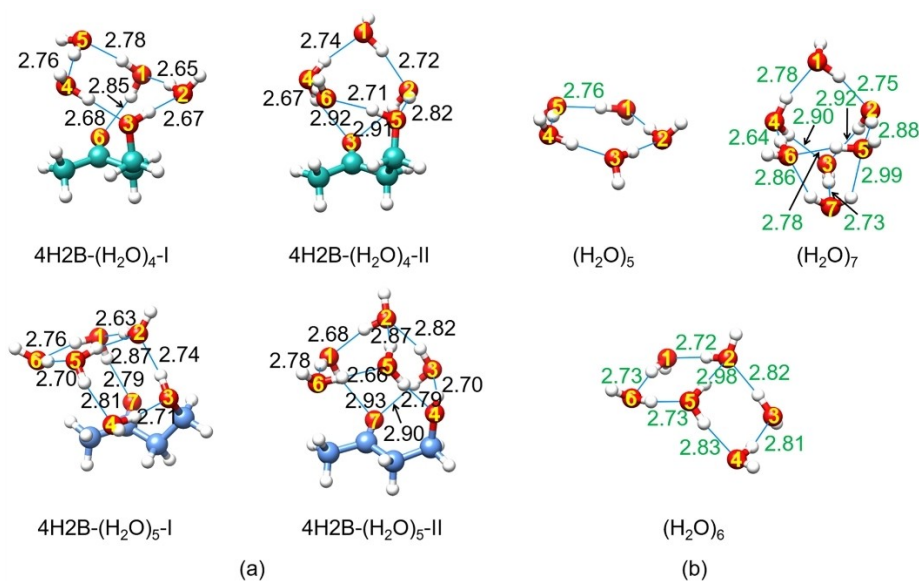


**Figure 3.** (a) The observed structures of 4H2B-(H<sub>2</sub>O)<sub>n=4-5</sub> indicating the theoretical values of the O...O distances (B3LYP-D3(BJ))/6-311++G(d,p). (b) The geometries and O...O distances (green) of the corresponding pure water clusters are given for comparison.<sup>[4-7]</sup>

closing the pentagonal hydroxyl ring notably depart from linearity. In the two isomers, the oxygen ring displays a bent structure reminiscent of a puckered five-membered ring ( $16^\circ$  in isomer I vs.  $20^\circ$  in the water pentamer), with the oxygen atoms departing from planarity ca.  $8\text{--}10^\circ$ . Isomer II shows larger bending, with the out-of-plane oxygen pointing away from the carbonyl group. Because of the second link to the carbonyl group, one or two molecules adopt a triple role as double proton donors and an acceptor, showcasing the great flexibility of the 4H2B moiety to provide tailored possibilities for water aggregation. Meanwhile, the solvation influence on the 4H2B monomer is more obvious compared to smaller hydrates, as important deformations are apparent in the carbon skeleton and the alcohol group, resulting in a folded conformation. Interestingly, the preferred anticlinal carbon skeleton ( $\tau(\text{O8C9-C10C11})$  ca.  $105\text{--}127^\circ$ ) and the *gauche* oxygen torsion ( $\tau(\text{C9C10-C11O12})$  ca.  $60^\circ$ ) change compared to the free monomer. In addition, the *gauche* oxygen torsion remains very similar in the two isomers, but the terminal hydroxyl group can reverse again the clockwise or anticlockwise alignment of the water molecules. As the complexity of the HB networks increases, it is easier to identify more intricate, three-dimensional binding topologies. A closer look at isomer II reveals a HB geometry similar to the one observed in the pure water heptamer. As shown in Figure 3, the alcohol and the carbonyl groups play the role of heptamer O5 and O3, respectively. Despite slight distortions are present, the O...O distances exhibit similar values in both complexes, which further sustains their structural similarities. Several views of the isomer II overlaid with the pure water pentamer and/or heptamer can be found in Figures S4 and S5.

The PES of the pentahydrate  $4\text{H2B}-(\text{H}_2\text{O})_5$  was surprisingly simpler, as the number of predicted minima reduced to six isomers (within  $5\text{ kJ mol}^{-1}$ ) upon adding the fifth water molecule, which made the isomeric assignments much easier. Two isomers were observed in the spectrum, with their structures identified to be isomers I and II in Figure 3 (a). The pentahydrate scaffolding is also initiated at the alcohol group, now offering comparison with the water hexamer. The pure water hexamer is characterized by three non-planar isomeric structures denoted cage, prism, and book, observed at 1:1:0.25 population ratios in a supersonic jet-expansion.<sup>[7]</sup> It is thus interesting to check if these 3D arrangements survive when one or more of the water units are replaced by an alcohol or equivalent functional groups. In isomers I and II, the OH group undertakes the position of the O3 and O4 water molecule of the book structure, respectively. Besides, one or two water molecules bind to the carbonyl group, locking the book arrangement to the aliphatic chain. Finally, the 4H2B carbon-chain skeleton exhibits remarkable flexibility to host the water molecules in the book scaffolding, adopting either a *gauche* ( $\tau(\text{O8C9-C10C11})$  ca.  $50^\circ$ ) or an antiperiplanar structure ( $\tau(\text{O8C9-C10C11})$  ca.  $5^\circ$ ), which are quite different to the tetrahydrate and instead move back to carbon chain conformations observed in some isomers of the smaller  $n=1\text{--}3$  clusters. Figure 3 shows the O...O distances for both isomers compared with the book isomer of the pure water hexamer.

In isomer I, the O1...O2, O2...O3, O3...O4 and O2...O5 distances of  $2.63\text{ \AA}$ ,  $2.74\text{ \AA}$ ,  $2.71\text{ \AA}$  and  $2.87\text{ \AA}$ , respectively, are ca.  $\sim 0.1\text{ \AA}$  shorter than the corresponding values in the book structure of the pure water hexamer. In isomer II, all O...O distances match those of the book structure with very small deviations (around  $\pm 0.05\text{ \AA}$ ), except for the distances of O3...O4, O5...O6, and O2...O5. Despite these small deviations arising from the presence of the solute, the structural similarities with the book isomer are remarkable. In order to gain further insight on the subtle differences between these two isomers, we performed a simple energy decomposition analysis. For both hydrates, we analyzed the contributions to the binding energy from the insertion of the hydroxy group in the HB network (O3 or O4) and the distortion of the monomer (negative contribution), compared to the monomer minimum energy conformation. The energy contributions were estimated at the RI-MP2/aug-cc-pVTZ level of theory (Tables S61 and S62). Our results show that while the distortion of the monomer is similar in both isomers ( $12.05\text{ kJ mol}^{-1}$  vs  $12.28\text{ kJ mol}^{-1}$  for I and II, respectively), the contribution of the remaining water units is significantly different for each cluster, with an energy difference of  $6.83\text{ kJ mol}^{-1}$  in favor of isomer I. This clearly shows how the water HB network in isomer II is more strained compared to the isolated pure water cluster and provides evidence of the large adaptability of water networks when solvating an organic molecule.

The effect of the deformation energy of the monomer upon solvation can be gauged by exploring the PES arising from the extended or folded conformations of the carbon backbone and the orientation of the OH group. As shown in Figure 4, a comparison of the observed conformations highlights how the monomer unit undergoes significant structural torsions as the stepwise addition of water takes place. The addition of further water molecules provides enough internal energy to circumvent the energy toll given by these distortions and thus higher energy forms become observable. As examples, the deformation energies between the

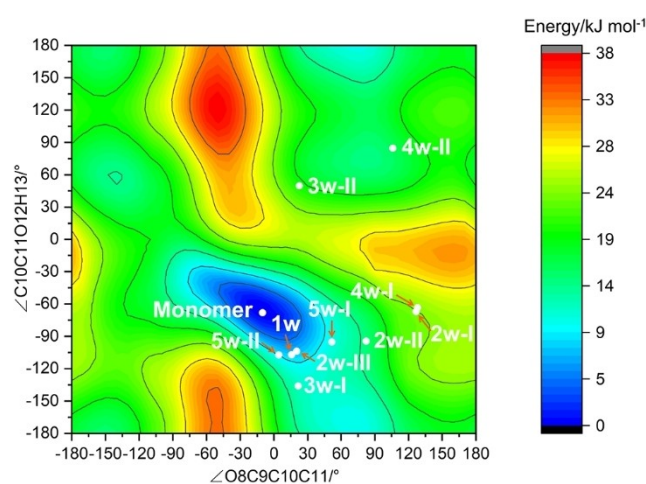


**Figure 4.** Relaxed PES scan for 4H2B along the dihedral angles  $\tau(\text{O8C9-C10C11})$  and  $\tau(\text{C10C11-O12H13})$ , the corresponding geometries of the 4H2B subunits in  $4\text{H2B}-(\text{H}_2\text{O})_{n=0-5}$  are indicated.

4H2B moiety in 4H2B-H<sub>2</sub>O and 4H2B-(H<sub>2</sub>O)<sub>4</sub>-II and the observed free monomer (Figure 2 (a)) are the smallest and largest identified, accounting for ~10 kJ mol<sup>-1</sup> and ~26 kJ mol<sup>-1</sup> (also in Figure S1), respectively. Thus, the water molecules can induce changes to a structure of 4H2B which is ~26 kJ mol<sup>-1</sup> higher in energy than the most stable conformer of the free monomer, stabilizing this structure in the complex.

The emerging picture is that molecular flexibility opens a larger variety of possibilities when creating the first solvation shell of an organic molecule. Before the present study, only molecules with reduced conformational flexibility had been reported at high resolution, such that several new conclusions can relevantly be drawn from our findings. First, in the case of small clusters, water molecules start inducing visible conformational changes of the 4H2B moiety in 4H2B-(H<sub>2</sub>O)<sub>2</sub>. As observed in isomer III of 4H2B-(H<sub>2</sub>O)<sub>2</sub>, the OH group can be inserted between two water molecules, deviating from the typical behavior of water dimerization commonly reported for other dihydrated clusters. Second, as the cluster size increases, the aggregation of water molecules in 4H2B-(H<sub>2</sub>O)<sub>n=3-5</sub> begins to resemble the pure water clusters, i.e. the 4H2B moiety's relative influence on the aggregation of water molecules decreases. Simultaneously, the conformational behavior of 4H2B becomes increasingly dependent on the water cluster's preferred structure. This is particularly evident in the two isomers of 4H2B-(H<sub>2</sub>O)<sub>4</sub>, where the 4H2B moiety must adjust three dihedral angles very differently to accommodate the water molecules. Third, the range of extension and the binding sites of the flexible molecule determine the extent of its structural changes and how the structural alterations are induced upon water aggregation.

Overall, the formation of the observed water aggregates is governed by a delicate energetic balance between distortions of the solute and water hydrogen bond networks. This energy balance plays a crucial role in the molecule's overall stability and potential reactivity caused by the presence of solvent molecules in the vicinity of the organic molecule. The large conformational flexibility of 4H2B enabled the observation of several isomers for each cluster size compared to the commonly reported observation of a single isomer in related studies on hydrated organic molecules. Our investigation serves as a first example that offers deeper insights into the conformational behavior of flexible molecules and their water clusters, particularly in scenarios where structural changes are essential for designing new materials and optimizing chemical processes in solution.

### Acknowledgements

M.L. and J.-U.G. gratefully thank for funding from the Deutsche Forschungsgemeinschaft (DFG, GR1344), as well as support from the Land Niedersachsen and Leibniz Universität IT Service (LUIS). W.L., C.P. and A.L. acknowledge funding from the Spanish *Ministerio de Ciencia e Innovación* and the *European Regional Development Fund* (MICINN-ERDF, Grant No. PID2021-125015NBI00) and

the *Junta de Castilla y León* (Grant Nos. INFRARED IR2021-UVa13 and IR2020-1-UVa02). M. L. and W.L. thank the *China Scholarship Council* for a research scholarship. Open Access funding enabled and organized by Projekt DEAL.

### Conflict of Interest

The authors declare no conflict of interest.

### Data Availability Statement

The data that support the findings of this study are provided in the Supporting Information of this article and are also available from the corresponding authors upon reasonable request.

**Keywords:** Conformational behavior · Water clusters · Non-covalent interactions · Hydrogen bonding · Rotational spectroscopy

- [1] F. H. Stillinger, *Science* **1980**, *209*, 451–457.
- [2] P. Ball, *Chem. Rev.* **2008**, *108*, 74–108.
- [3] B. Bagchi, *Water in Biological and Chemical Processes: From Structure and Dynamics to Function*, Cambridge Univ. Press, Cambridge, UK **2013**.
- [4] J. D. Cruzan, L. B. Braly, K. Liu, M. G. Brown, J. G. Loeser, R. J. Saykally, *Science* **1996**, *271*, 59–62.
- [5] K. Liu, M. G. Brown, J. D. Cruzan, R. J. Saykally, *Science* **1996**, *271*, 62–64.
- [6] F. N. Keutsch, R. J. Saykally, *Proc. Nat. Acad. Sci.* **2001**, *98*, 10533–10540.
- [7] C. Pérez, M. T. Muckle, D. P. Zaleski, N. A. Seifert, B. Temelso, G. C. Shields, Z. Kisiel, B. H. Pate, *Science* **2012**, *336*, 897–901.
- [8] C. Pérez, S. Lobsiger, N. A. Seifert, D. P. Zaleski, B. Temelso, G. C. Shields, Z. Kisiel, B. H. Pate, *Chem. Phys. Lett.* **2013**, *571*, 1–15.
- [9] C. Pérez, D. P. Zaleski, N. A. Seifert, B. Temelso, G. C. Shields, Z. Kisiel, B. H. Pate, *Angew. Chem. Int. Ed.* **2014**, *53*, 14368–14372.
- [10] K. E. Otto, Z. Xue, P. Zielke, M. A. Suhm, *Phys. Chem. Chem. Phys.* **2014**, *16*, 9849–9858.
- [11] G. E. Douberly, R. E. Miller, S. S. Xantheas, *J. Am. Chem. Soc.* **2017**, *139*, 4152–4156.
- [12] B. Guillot, *J. Mol. Liq.* **2002**, *101*, 219–260.
- [13] L. Evangelisti, W. Caminati, *Phys. Chem. Chem. Phys.* **2010**, *12*, 14433–14441.
- [14] D. H. Wertz, H. A. Scheraga, *Macromolecules* **1978**, *11*, 9–15.
- [15] Y. M. Rhee, E. J. Sorin, G. Jayachandran, E. Lindahl, V. S. Pande, *Proc. Nat. Acad. Sci.* **2004**, *101*, 6456–6461.
- [16] J. E. Ladbury, *Chem. Biol.* **1996**, *3*, 973–980.
- [17] J. Schiebel, R. Gaspari, T. Wulsdorf, K. Ngo, C. Sohn, T. E. Schrader, A. Cavalli, A. Ostermann, A. Heine, G. Klebe, *Nat. Commun.* **2018**, *9*, 3559.
- [18] M. Becucci, S. Melandri, *Chem. Rev.* **2016**, *116*, 5014–5037.
- [19] S. T. Shipman, B. H. Pate, in *Handbook High-Resolution Spectroscopy* (Eds.: F. Merkt, M. Quack), John Wiley & Sons, Ltd, New York **2011**, pp. 801–828.

- [20] J.-U. Grabow, in *Handbook High-Resolution Spectroscopy* (Eds.: F. Merkt, M. Quack), John Wiley & Sons, Ltd, New York **2011**, pp. 723–799.
- [21] W. Caminati, J.-U. Grabow, in *Frontiers and Advances in Molecular Spectroscopy*, Elsevier Inc. **2018**, pp. 569–598.
- [22] W. Sun, M. Schnell, *Angew. Chem. Int. Ed.* **2022**, *61*, e202210819.
- [23] W. Li, C. Pérez, A. L. Steber, M. Schnell, D. Lv, G. Wang, X. Zeng, M. Zhou, *J. Am. Chem. Soc.* **2023**, *145*, 4119–4128.
- [24] A. L. Steber, B. Temelso, Z. Kisiel, M. Schnell, C. Pérez, *Proc. Nat. Acad. Sci.* **2023**, *120*, e2214970120.
- [25] C. J. Gruenloh, J. R. Carney, C. A. Arrington, T. S. Zwier, S. Y. Fredericks, K. D. Jordan, *Science* **1997**, *276*, 1678–1681.
- [26] R. N. Pribble, T. S. Zwier, *Science* **1994**, *265*, 75–79.
- [27] D. P. Tabor, R. Kusaka, P. S. Walsh, E. L. Sibert, T. S. Zwier, *J. Phys. Chem. Lett.* **2015**, *6*, 1989–1995.
- [28] A. S. Hazrah, A. Insausti, J. Ma, M. H. Al-Jabiri, W. Jäger, Y. Xu, *Angew. Chem. Int. Ed.* **2023**, *62*, e202310610.
- [29] C. Pérez, J. C. López, S. Blanco, M. Schnell, *J. Phys. Chem. Lett.* **2016**, *7*, 4053–4058.
- [30] J. Thomas, O. Sukhorukov, W. Jäger, Y. Xu, *Angew. Chem. Int. Ed.* **2014**, *53*, 1156–1159.
- [31] M. J. Tubergen, C. R. Torok, R. J. Lavrich, *J. Chem. Phys.* **2003**, *119*, 8397–8403.
- [32] T. A. Legreve, W. H. James III, T. S. Zwier, *J. Phys. Chem. A* **2009**, *113*, 399–410.
- [33] Y. Yang, M. Alshalafeh, Y. Xu, *Spectrochim. Acta Part A* **2024**, *307*, 123634.
- [34] M. Li, Y. Zheng, J. Li, J.-U. Grabow, X. Xu, Q. Gou, *Phys. Chem. Chem. Phys.* **2022**, *24*, 19919–19926.
- [35] J. L. Neill, S. T. Shipman, L. Alvarez-Valtierra, A. Lesarri, Z. Kisiel, B. H. Pate, *J. Mol. Spectrosc.* **2011**, *269*, 21–29.
- [36] A. Lesarri, R. Pinacho, L. Enríquez, J. E. Rubio, M. Jaraíz, J. L. Abad, M. A. Gigosos, *Phys. Chem. Chem. Phys.* **2017**, *19*, 17553–17559.
- [37] S. Grimme, C. Bannwarth, P. Shushkov, *J. Chem. Theory Comput.* **2017**, *13*, 1989–2009.
- [38] A. D. Becke, *J. Chem. Phys.* **1993**, *98*, 1372–1377.
- [39] S. Grimme, J. Antony, S. Ehrlich, H. Krieg, *J. Chem. Phys.* **2010**, *132*.
- [40] S. Grimme, S. Ehrlich, L. Goerigk, *J. Comput. Chem.* **2011**, *32*, 1456–1465.
- [41] R. Krishnan, J. S. Binkley, R. Seeger, J. A. Pople, *J. Chem. Phys.* **1980**, *72*, 650–654.
- [42] F. Weigend, R. Ahlrichs, *Phys. Chem. Chem. Phys.* **2005**, *7*, 3297–3305.
- [43] A. Schäfer, C. Huber, R. Ahlrichs, *J. Chem. Phys.* **1994**, *100*, 5829–5835.
- [44] S. Grimme, F. Neese, *J. Chem. Phys.* **2007**, *127*.
- [45] F. Weigend, M. Häser, *Theor. Chem. Acc.* **1997**, *97*, 331–340.
- [46] F. Weigend, M. Häser, H. Patzelt, R. Ahlrichs, *Chem. Phys. Lett.* **1998**, *294*, 143–152.
- [47] R. A. Distasio, R. P. Steele, Y. M. Rhee, Y. Shao, M. Head-Gordon, *J. Comput. Chem.* **2007**, *28*, 839–856.
- [48] Gaussian 16, Revision B.01, M. J. Frisch, G. W. Trucks, H. B. Schlegel, G. E. Scuseria, M. A. Robb, J. R. Cheeseman, G. Scalmani, V. Barone, G. A. Petersson, H. Nakatsuji, M. Caricato, A. V. Marenich, J. Bloino, B. G. Janesko, R. Gomperts, B. Mennucci, H. P. Hratchian, J. V. Ortiz, A. F. Izmaylov, J. L. Sonnenberg, D. Williams-Young, F. Hing, F. Lipparini, F. Egidi, J. Goings, B. Peng, A. Petrone, T. Henderson, D. Ranasinghe, V. G. Zakrzewski, J. Gao, N. Rega, G. Zheng, W. Liang, M. Hada, M. Ehara, K. Toyota, R. Fukuda, J. Hasegawa, M. Ishida, T. Nakajima, Y. Honda, O. Kitao, H. Nakai, T. Vreven, K. Throssell, J. A. Jr Montgomery, J. E. Peralta, F. Ogliaro, M. J. Bearpark, J. J. Heyd, E. N. Brothers, K. N. Kudin, V. N. Staroverov, T. A. Keith, R. Kobayashi, J. Normand, K. Raghavachari, A. P. Rendell, J. C. Burant, S. S. Iyengar, J. Tomasi, M. Cossi, J. M. Millam, M. Klene, C. Adamo, R. Cammi, J. W. Ochterski, R. L. Martin, K. Morokuma, O. Farkas, J. B. Foresman, D. J. Fox, Gaussian, Inc., Wallingford USA **2016**.
- [49] F. Neese, *Wiley Interdiscip. Rev.: Comput. Mol. Sci.* **2022**, *12*, e1606.
- [50] J. K. G. Watson, in *Vib. Spectra Struct. Vol. 6* (Ed.: J. R. Durig), Elsevier B. V., Amsterdam **1977**, pp. 1–89.
- [51] J. Kraitchman, *Am. J. Phys.* **1953**, *21*, 17–24.
- [52] H. D. Rudolph, J. Demaison, in *Equilibrium Molecular Structures* (Ed.: A. Demaison, J. Boggs, J. Császár), CRC Press, Boca Raton, FL **2011**, pp. 125–158.
- [53] J. Vazquez, J. F. Stanton, in *Equilibrium Molecular Structures* (Eds.: J. Demaison, J. E. Boggs, A. Császár), CRC Press, Boca Raton, Florida **2011**, pp. 53–88.

Manuscript received: March 5, 2024

Accepted manuscript online: May 8, 2024

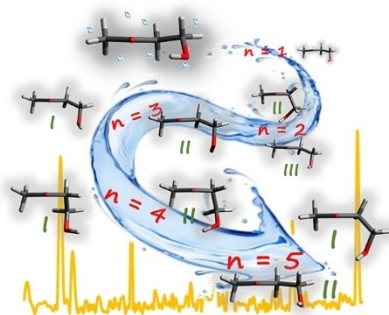
Version of record online: ■■■■■

## Communications

## Microsolvation

M. Li, W. Li, C. Pérez, A. Lesarri,\* J.-  
U. Grabow\* [e202404447](#)

Adaptive Response to Solvation in Flexible  
Molecules: Oligo Hydrates of 4-Hydroxy-2-  
butanone



Stepwise Hydration of a flexible organic molecule reveals how water solvation scaffolds deforms the substrate structure, generally through different structural pathways. In this experiment we observed solvation with up to five water molecules for 4-hydroxy-2-butanone, using broadband microwave spectroscopy. Solvation is accompanied by multiple isomerization, as two isomers were rotationally detected for each cluster.